Microwave-Assisted Switching of Microscopic Rings: Correlation Between Nonlinear Spin Dynamics and Critical Microwave Fields

Jan Podbielski* and Detlef Heitmann

Institut für Angewandte Physik und Mikrostrukturforschungszentrum, Universität Hamburg, Jungiusstrasse 11, D-20355 Hamburg, Germany

Dirk Grundler†

Physik-Department E10, Fakultät für Physik, Technische Universität München, James-Franck-Strasse, D-84748 Garching, Germany

(Received 25 July 2007; published 14 November 2007)

We have studied the spin dynamics of microscopic permalloy rings at GHz frequencies. Increasing the irradiation power, we observe first nonlinear spin dynamics and second microwave-assisted switching (MAS). We explore the MAS phase diagram as a function of microwave power and frequency f and, in particular, extract the critical microwave field $h_c(f)$. Its frequency dependence reflects characteristic eigenfrequencies from both the linear and nonlinear spin-wave spectrum. By comparing $h_c(f)$ with the different susceptibilities, we gain insight into the microscopic processes which might be the basis of a predictive theory of MAS.

DOI: 10.1103/PhysRevLett.99.207202 PACS numbers: 75.40.Gb, 75.75.+a, 76.50.+g

Following the pioneering work of Thirion *et al.* on magnetic nanocrystals [1], there is a growing interest in switching of magnetic devices by microwave irradiation. It has been argued that an rf frequency f that matches the eigenfrequency of the uniform spin precession initiates the switching. Very recently, it has been reported, however, that high microwave powers change the spin-wave modes in thin-film magnets [2,3]. So far, these two intriguing experiments in the nonlinear spin dynamics regime have been conducted separately and on samples of considerably different lateral size. For a microscopic magnet with a certain domain configuration, the fundamental link between spin dynamics and switching in the presence of microwave irradiation is even completely missing. Microwave assisted switching (MAS) might become technologically relevant like thermally assisted magnetic recording, already explored for hard disk drives.

We have investigated the spin dynamics of nanostructured permalloy ($Ni_{80}Fe_{20}$) rings exhibiting a tailored quasistatic magnetization configuration [4–7]. The so-called vortex state allows us to address spin wave modes, both, confined to a small ring segment (modes A') or extending in azimuthal direction along the ring (modes I_n) [8–13] for the MAS process. We will demonstrate that a high microwave power has a manyfold impact: (i) it provokes a distinct change of the spin wave modes, (ii) produces a frequency-dependent instability in the magnetization state and (iii) initiates the transition to the reversed state, i.e., the reversed onion state. In contrast to the previous works on nanocrystals [1] and on macroscopic ellipsoids [14], we find that the threshold for MAS, i.e., the *critical microwave field* $h_c(f)$, forms a complex spectrum and does not show a one-to-one correspondence with the spin wave spectrum neither in the linear nor in the nonlinear regime. We discuss possible microscopic mechanisms. However, a quantitative theory for the MAS process in mesoscopic magnets needs to be developed.

Broadband spin wave spectroscopy has been performed on two different samples, each consisting of 20 nominally identical permalloy rings integrated to the central conductor of a coplanar wave guide (CPW). The fabrication and experimental technique have been described elsewhere [8,9]. The rings of both samples had an outer diameter $D = 2200 \pm 100$ nm, a thickness $t = 25 \pm 4$ nm, and a ring-to-ring separation of 450 ± 30 nm. The samples differed intentionally by the ring widths $w = 500 \pm 30$ nm (sample 1) and $w = 700 \pm 30$ nm (sample 2). Such rings were known to exhibit similar domain configurations but different quasistatic switching fields H^s [15] and, what will be even more important, different spin wave eigenfrequencies and mode patterns [9,16]. The relative transmission T was measured at room temperature by means of a vector network analyzer (VNA) connected to the CPW. The power P ranged from 100 μW to 75 mW using a separate microwave amplifier and microwave switches. In the CPW, the amplitude of the rf field h_{rf} was up to $\mu_0 h_{\mathrm{rf}} = \mu_0\sqrt{\frac{P}{2Z_0 w_{\mathrm{CPW}}^2}} = 12.4$ mT at $P = 75$ mW with $Z_0 = 50\ \Omega$ and $w_{\mathrm{CPW}} = 2800 \pm 100$ nm (width of the central conductor) [17]. The excited spin waves induced the absolute voltage V_{ind} in the CPW from which we calculated the magnetic susceptibility χ following Refs. [16,17]. A static external magnetic field $\mu_0 H$ (of up to 90 mT) was applied parallel to the CPW, i.e., orthogonal to h_{rf}.

In Fig. 1(a), we summarize transmission spectra recorded on sample 1 ($w = 500$ nm) at different in-plane fields with $-24\ \mathrm{mT} \leq \mu_0 H \leq 0$. The VNA output power $P = -10$ dBm $= 100\ \mu$W is small, and the magnetization dynamics are in the linear regime. The rings are found to exhibit the typical reversal behavior with two switching fields [4,6,7]: for $\mu_0 H \geq \mu_0 H_1^s = -0.9$ mT and

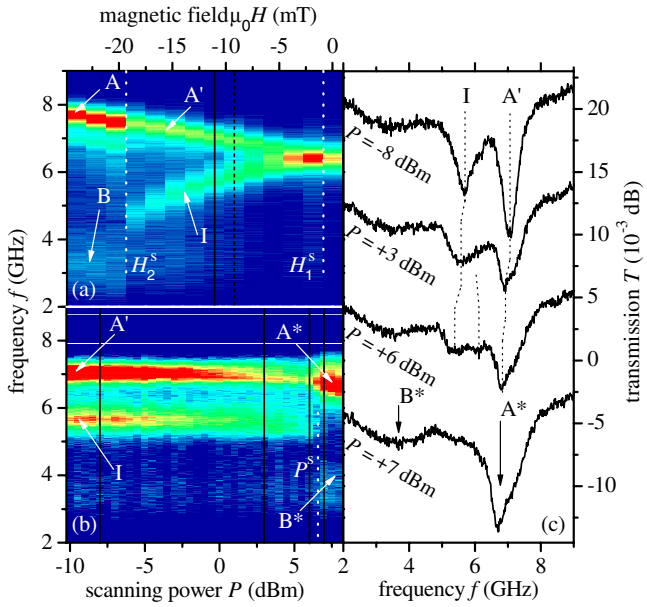

FIG. 1 (color online). Color-scaled absorption spectra taken on rings with $w = 500$ nm at (a) constant VNA power $P = -10$ dBm and successively decreasing magnetic field, (b) constant field $\mu_0 H = -11.1$ mT (initializing the vortex state) for increasing VNA output power P. Labels highlight strong absorption (spin wave eigenmodes). In (a), spectra were taken after saturation at $\mu_0 H = +90$ mT. Here, white dotted vertical lines indicate switching fields. Modes A', I (A, B) are characteristic for the vortex (onion) state. [8] In (b), modes A^* and B^* indicate that microwave assisted switching into the onion state has occurred beyond $P^s \geq 6.5$ dBm (vertical dotted line). (c) Individual spectra extracted from (b) at the depicted black vertical lines. Spectra are offset for clarity.

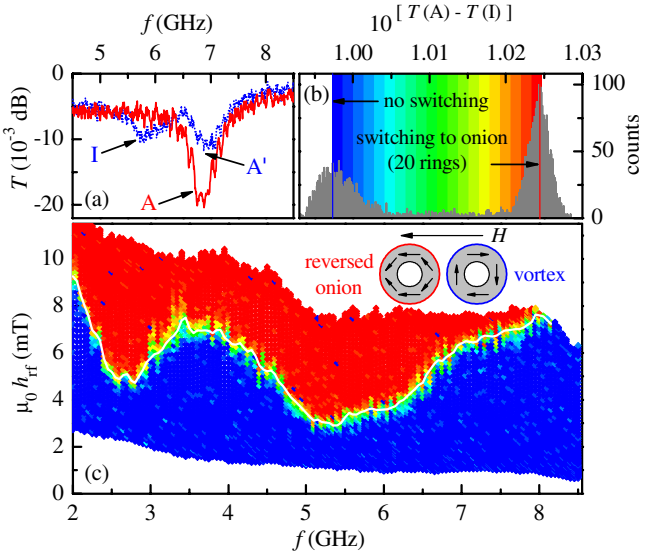

FIG. 2 (color online). (a) Spectra measured at $P = -10$ dBm and $\mu_0 H = -9.2$ mT *after* two different irradiation experiments performed at $\mu_0 H = -11.1$ mT: full line—$f = 2$ GHz, $P = 75$ mW, and $\mu_0 h_{rf} = 12.4$ mT, the rings switched to the reversed *onion* state; dotted line—$f = 8.5$ GHz, $P = 0.2$ mW, and $\mu_0 h_{rf} = 0.7$ mT, the rings remained in the *vortex* state. (b) Histogram summarizing all the evaluated peak differences in 8450 MAS experiments performed on sample 1. (c) Phase diagram for switching to the reversed onion state (above) from the vortex state (below the white line) at $\mu_0 H = -11.1$ mT. The magnetization states and orientation of H are illustrated in the inset. The white line indicates the phase boundary (critical microwave field) $h_c(f)$ where more than 10 rings have switched.

$\mu_0 H \leq \mu_0 H_2^s = -19.4$ mT, the rings are in the onion and reverse onion state, respectively [cf. inset of Fig. 2(c)]. The magnetization M of both ring halves is *parallel* to H with domain walls in the head and tail. Here, modes A and B [see labels in Fig. 1(a)] are prominent. They originate from localized spin wave excitations: mode A resides in the ring segments where H is tangential, and mode B is at the domain walls. [7–10] Lowering H below H_1^s makes the rings switch to the vortex state, where spins are aligned with each other and follow the ring's edges. No domain wall is present [cf. inset in Fig. 2(c)]. For $H_1^s > H > H_2^s$, we distinguish the azimuthal mode I and the localized mode A' [12]. The former consists of a set of discrete modes I_n ($n = 1, 2, \ldots$) which are known to follow a field dispersion with negative slope [11,12]. Modes I_n exhibit spin wave antinodes in the ring half where H and M are oriented in particular *antiparallel* [11]. In contrast, the mode A' is localized in the ring segment where H and M are oriented in *parallel*, similar to mode A of the onion state. Modes A' and A are only offset by a frequency shift of 200 MHz as seen in Fig. 2(a) where we compare spectra at the same field value $|\mu_0 H| = 9.3$ mT in the vortex (dotted line) and the onion (solid line) state measured at $P = -10$ dBm. Later, we will use the transmission T of the characteristic resonances shown in Fig. 2(a) to quantify the number of rings that are in the vortex and onion state, respectively.

In Figs. 1(b) and 1(c), we now depict the spin wave absorption as a function of VNA output power P at $\mu_0 H = -11.1$ mT $> H_2^s$ [cf. black solid vertical in Fig. 1(a)]. In the following, we distinguish three regimes. In regime (1), i.e., the linear regime for $P < -5$ dBm $= 300$ μW ($\mu_0 h_{rf} \leq 0.8$ mT), modes A' and I of the vortex state are well resolved. The eigenfrequencies do not vary. For -5 dBm $< P < +6$ dBm [regime (2)], the spectra exhibit five characteristic changes with increasing P [cf. Figure 1(c)]: (i) modes A' and I first shift to *smaller* frequencies f, (ii) their intensities decrease, and (iii) line widths increase. (iv) The resonances become asymmetric, and (v) mode I is found to split up into further absorption lines I_n, each with a distinct power dependence. We attribute regime (2) to nonlinear spin dynamics that are due to large spin-precession angles. For ferromagnetic resonances, it was shown that a magnet's shape and orientation in an external field H played an important role for the observed frequency shifts [18–20]. For example, the uni-

form mode of a macroscopic disk was found to shift to *smaller* (larger) f with increasing P if H was oriented *parallel* (perpendicular) to the *easy plane* [19]. For our microscopic magnets, we observe in Fig. 1(b) that the frequency of A' becomes *smaller*. This behavior is consistent with A' being localized in a ring segment where the magnetization M is parallel to the *easy direction*. Consistently, we find a similar shift for mode A in the onion state, labeled A^* in Fig. 1(b) for the high power level. For $P \geq P^s = +6.5 \pm 0.4$ dBm [regime (3)], the spectra change even more drastically. Beyond P^s (critical output power), we detect two modes A^*, B^*, and no longer mode I. At $P = 7$ dBm, these modes are found at 6.7 and 3.6 GHz, respectively. Power dependent measurements at $\mu_0 H = 11.1$ mT (not shown) confirm that the observed modes A* and B* are characteristic for the *onion state* and the counterparts of modes A and B [8]. A high VNA output power thus changes the quasistatic magnetization configuration. We have observed the same microwave-assisted switching on sample 2 exhibiting a smaller $|H_2^s|$ and P^s due to the larger ring width $w = 700$ nm. Heating of the central part of the CPW is ruled out to cause the switching. We measured the CPW's temperature rise to be, e.g., only 5 K (2 K) for 75 mW at 2 GHz (13 mW at 5.4 GHz). For the following discussion on the microscopic origin of MAS, it is instructive to consider magnetic susceptibilities $\chi(f)$. In Fig. 3, $\chi(f)$ is depicted for rings with (a) $w = 500$ nm and (b) $w = 700$ nm. We compare χ at $P = -8$ dBm (linear regime, light gray curves) and $P = +6$ dBm $< P^s$ (nonlinear regime, dark gray curves). χ_0 denotes the susceptibility in the linear regime. Increasing P decreases the magnetic susceptibility and broadens the resonant peaks. In Fig. 3(a), three broad maxima are found near 3, 5.5 and 7.1 GHz. At resonance and $P \leq P^s$, each ring absorbs a power of ≤ 1 μW, and the intrinsic temperature rise is far below 1 K.

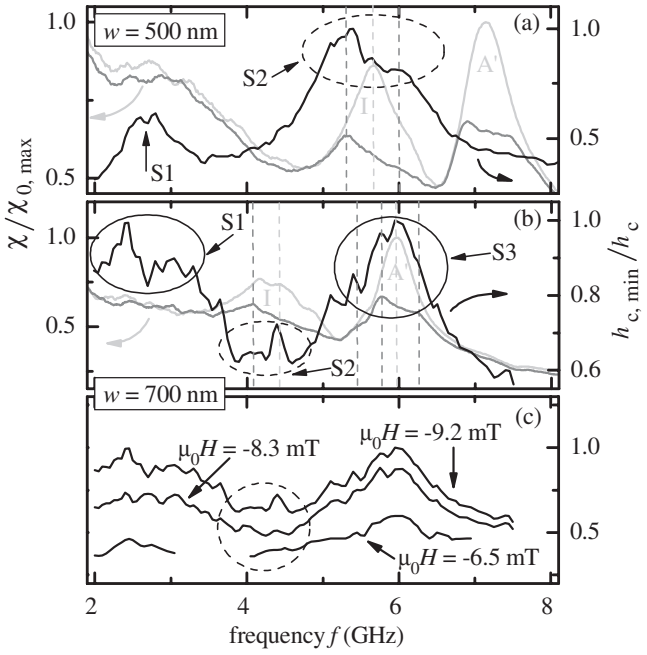

FIG. 3. (a,b) Inverse critical microwave field $h_{c,\min}/h_c$ (black) compared to magnetic susceptibilities χ (gray) measured via broadband VNA transmission spectroscopy for (a) 500 nm at -11.1 mT and (b) 700 nm wide rings at -9.2 mT. (c) $h_{c,\min}/h_c$ for different static fields H in the vortex state of sample 2, i.e., for different effective energy-barrier heights. Labels are explained in the text.

To investigate the power and frequency dependence of the MAS process in detail, we change the experiment. For this, we irradiate the rings at $\mu_0 H = -11.1$ mT in the vortex state with $h_{\rm rf}$ at a single frequency f before we measure the spin wave spectrum at *small* VNA output power $P = -10$ dBm, i.e., in the *linear* regime, at $\mu_0 H = -9.2$ mT [black dashed vertical in Fig. 1(a)]. We choose a duration of 300 ms to study MAS for steady-state spin precession. The experiment is repeated for different amplitudes $h_{\rm rf}$ and f. By this means, we explore the phase diagram as shown in Fig. 2(c). To quantify the switching process, we have calculated the number of rings in the two quasistatic magnetization configurations from the absolute signal strength T of modes A (onion state) and I (vortex state) [cf. Figure 2(a)]. To calibrate the peak differences $T(A)$-$T(I)$, we use the histogram in Fig. 2(b). It summarizes all the evaluated peak differences on a linear scale forming the phase diagram in Fig. 2(c): the two pronounced maxima reflect 20 rings being all either in the vortex (no switching) or onion state (20 rings have switched). Peak differences lying in between reflect the array exhibiting a distribution of both states. The color-coding of $10^{[T(A)-T(I)]}$ provides the exact number of reversed rings.

In Fig. 2(c), we show the data from a series of 8450 individual microwave-irradiation experiments performed on rings of $w = 500$ nm. We observe that the rings are stable in the vortex state only for parameters below the white full line in Fig. 2(c). At this phase boundary, $h_{\rm rf}$ reaches a critical value h_c where ten rings or more switch irreversibly to the onion state. We find that the frequency dependence of the critical microwave field h_c is complex and resembles a spectrum with characteristic minima. In the global minimum, the switching process is stimulated by $\mu_0 h_{\rm rf}$ of only 3 mT. Note that the field $h_{\rm rf}$ is oriented perpendicular to the CPW. If we add $|\mu_0 H| = |-11.1|$ mT and $h_{\rm rf}$ considering the different orientations, we end up with an effective field amplitude $\mu_0\sqrt{H^2 + h_{\rm rf}^2} = 11.5$ mT. The ring geometry allows us to directly compare this value with the quasistatic switching field $|\mu_0 H_2^s| = 19.4$ mT. In case of ideal radial symmetry, H_2^s is independent of the field orientation [5,6]. For a single-domain Stoner-Wohlfarth particle or a rectangular magnet, the direct comparison would not be feasible. Their switching fields are angle dependent. Our data show that the dynamical switching field is smaller than the quasistatic one by 40%. This comparison confirms the antici-

pated resonant behavior of the MAS process. At the phase boundary $h_c(f)$, the dynamic magnetization reaches a frequency-dependent critical amplitude $m_c(f)$ and stimulates the ring's reversal.

In the following, we calculate $h_{c,\min}/h_c$ [black curve in Fig. 3(a)] which we will call switching spectrum (SSp) for brevity. On the one hand, the inverse quantity $1/h_c$, normalized by multiplying with the minimum h_c, allows us to identify resonant features as pronounced peaks [cf. $\chi(f)$]. On the other hand, if the correct variation of $m_c(f)$ with frequency would be known, the term $m_c(1/h_c)$ might be interpreted as a susceptibility and could be compared quantitatively with $\chi(f)$ obtained from broadband VNA transmission spectra. This however rests to a microscopic theory which still needs to be developed as argued below. For the resonances in Fig. 3(a), we observe a close correlation between $h_{c,\min}/h_c$ and χ only in the range from 5 to 6.5 GHz. The feature S2 of the SSp in Fig. 3(a) consists of three distinct resonances highlighted by the dashed vertical lines. We conclude that S2 reflects spin wave eigenfrequencies of azimuthal modes I_n from both the linear and nonlinear regime. Their spin precession amplitudes have been reported to be largest where the magnetization is oriented antiparallel to H [11]. Excitation of these modes thus stimulates the reversal accompanied by domain wall nucleation. The correlation of feature S2 with χ at $P = +6$ dBm in the nonlinear regime suggests that MAS is triggered directly by the spin precession amplitude. Interestingly, mode A' which is localized where the magnetization is already aligned with H is not observed in the SSp. The feature S1 residing at small frequency f does not have a pronounced counterpart in χ. This might be a soft mode of the vortex state that obeys a small absorption coefficient and is resolved only as a broad peak at $f <$ 4 GHz in the transmission spectrum. We suppose the soft mode to be an edge mode localized in the ring's head and tail similar to mode B of the onion state.

In Fig. 3(b), we find for 700 nm wide rings (sample 2) three distinct features in the SSp. S1 and S2 are consistent with sample 1. However, we observe an additional feature S3 that reflects eigenfrequencies of the localized mode A' in both the linear and nonlinear regime. Counterintuitively, mode A' for which M is (already) parallel to H is most efficient for the MAS process. Reasons might be that in case of a large w, the spin wave pattern exhibits long tails extending over the whole rings [16] and that the high excitation power leads to a further modification of the mode profile [2]. The dominance of mode A' is in contrast to Ref. [14] where, in macroscopic ellipsoids, a soft mode was efficient. The feature S2 originating from modes I_n is small for $w = 700$ nm. To investigate this further, we have measured the SSp at three different H [Fig. 3(c)]. Through H, we define the effective energy-barrier height. When H approaches H_2^s, the barrier height is reduced and $h_{c,\min}/h_c$ overall increases. At the same time, the features S1 and S2 become more pronounced which belong to a soft mode and to the spin wave excitation in the antiparallel ring half, respectively. To understand such a complex behavior on a quantitative level, a theoretical model for the MAS process needs to be developed. Note that mode A' which exhibits the largest absorption in the linear regime is missing in the SSp of Fig. 3(a). A pure bolometric process for MAS is thus ruled out.

In conclusion, using broadband spin wave spectroscopy, we have investigated in detail the microwave assisted switching of rings. Three different kinds of spin wave modes were shown to contribute to the MAS process which might be technologically relevant. Microscopic magnets in different magnetization states could be reversed resonantly and addressed individually. This is different from thermally assisted magnetic recording.

The authors are grateful to F. Giesen, B. Botters, and D. Görlitz for discussions and experimental support. Financial support by the DFG via No. SFB668 and the excellence cluster Nanosystems Initiative Munich is acknowledged.

*jpodbiel@physnet.uni-hamburg.de
†grundler@ph.tum.de

[1] C. Thirion, W. Wernsdorfer, and D. Mailly, Nat. Mater. **2**, 524 (2003).
[2] V. E. Demidov, U.-H. Hansen, and S. O. Demokritov, Phys. Rev. Lett. **98**, 157203 (2007).
[3] T. Gerrits *et al.*, Phys. Rev. Lett. **98**, 207602 (2007).
[4] J. Rothman *et al.*, Phys. Rev. Lett. **86**, 1098 (2001).
[5] M. Kläui *et al.*, Appl. Phys. Lett. **84**, 951 (2004).
[6] H. Rolff, W. Pfützner, Ch. Heyn, and D. Grundler, J. Magn. Magn. Mater. **272–276**, 1623 (2004).
[7] J. Podbielski *et al.*, Superlattices Microstruct. **37**, 341 (2005).
[8] F. Giesen *et al.*, Appl. Phys. Lett. **86**, 112510 (2005).
[9] F. Giesen *et al.*, J. Appl. Phys. **97**, 10A712 (2005).
[10] I. Neudecker *et al.*, Phys. Rev. Lett. **96**, 057207 (2006).
[11] X. Zhu *et al.*, J. Appl. Phys. **99**, 08F307 (2006).
[12] J. Podbielski, F. Giesen, and D. Grundler, Phys. Rev. Lett. **96**, 167207 (2006).
[13] G. Gubbiotti *et al.*, Phys. Rev. Lett. **97**, 247203 (2006).
[14] H. T. Nembach *et al.*, Appl. Phys. Lett. **90**, 062503 (2007).
[15] Y. G. Yoo *et al.*, Appl. Phys. Lett. **82**, 2470 (2003).
[16] F. Giesen, J. Podbielski, and D. Grundler, Phys. Rev. B (to be published).
[17] T. J. Silva, C. S. Lee, T. M. Crawford, and C. T. Rogers, J. Appl. Phys. **85**, 7849 (1999).
[18] R. W. Damon, Rev. Mod. Phys. **25**, 239 (1953).
[19] N. Bloembergen and S. Wang, Phys. Rev. **93**, 72 (1954).
[20] H. Suhl, J. Phys. Chem. Solids **1**, 209 (1957).